Journal of the Nigerian Association of Mathematical Physics
Volume **23 (March, 2013), pp 325 – 334**

The Effect of Soot in the Radiative Forcing of Urban Aerosols

[1]Tijjani B. I. and [2]Akpootu D. O.
[1]Department of Physics,
Bayero Univerisity, Kano,
[2]Department of Physics,
Usmanu Danfodiyo University, Sokoto.

Abstract

In this paper extracted used data from Optical Properties of Aerosols and Cloud(OPAC) to model the effect of soot on optical depth, scattering and extinction coefficients, and asymmetry parameters at spectral range of 0.25 to 1.00 μm at eight different relative humidity (RH) (0, 50, 70, 80, 90, 95, 98 and 99%). The concentrations of soot were varied while those of water soluble and insoluble were kept constant. Using regression analysis, the Angstrom exponents were determined along with α_1 and α_2, the coefficients of a second order polynomial fit. The Angstrom coefficient increases with RH from 0-90%RH and decreases from 95-99% RH but $\alpha_1$is negative and continued to increase with the increase in both soot and RH, while α_2 which signifies curvature is positive at 0% RH and decreases with the increase in soot but negative as from 50 to 99% and increases in magnitude with the increase in soot and RH. The above optical parameters were also used to determine the radiative forcing. The relation of RadiativeForcing (RF) with wavelength is such that it decreases with power law as from 0 to 90% but quadratic from 95 to 99%. The effect of RH on RF(warming) is such that it decreases with RH. The effect of adding soot leads to increase in warming.

1.0 Introduction

A significant fraction of atmospheric aerosols is comprised of carbonaceous materials, which are often categorized as elemental or black/graphitic carbon (EC/BC) and organic carbon (OC) known as Carbonaceous particles which are a by-product of liquid or gaseous fuel combustion and are also known as soot [1]. Black carbon(BC) is produced as primary particles from incomplete combustion processes, in particular from diesel engines, which are the major source of black carbon in urban areas [2]. Soot particles are also produced in fuel-rich flames, or fuel rich parts of frames, as a result of incomplete combustion of carbonaceous fuel (of fossil fuels, biomass and agricultural wastes and forest fires) [3]. These forms of carbon play an important role in climate change, either contributing to or offsetting atmospheric warming [4, 5]. BC has attracted special attention because of its contribution to radiative heating [2, 6]. The Intergovernmental Panel on Climate Change (IPCC) has estimated that the global mean clear-sky radiative forcing of BC is 0.23 ± 0.25 Wm^{-2}[7], which is approximately half the value of Methane, the second most important greenhouse gas after Carbon dioxide. BC may also have regional climatic impacts. For example, Menon et. al. [5] have suggested that the high concentrations of soot over India and China are responsible for a trend toward increased flooding in the south and drought in the north. It is estimated that the reduced atmospheric transparency caused by high soot concentrations over India and China decreases agricultural productivity by 10–20% [8]. Soot deposited on plant leaves also reduces plant productivity [9]. In urban areas, black carbon is the principle particle species that absorbs radiation in the visible spectrum.

Soot consists of nearly monodispersed spherical particles that collect into mass fractal aggregates having a broad size distribution. The primary soot particles are usually very small. By combustion of gaseous or liquid fuel, the diameters of primary soot particles are usually in the range between 5 and 80 nm. Airborne soot and soot-containing aerosols are important components of the atmosphere [10, 11].

Understanding the influence of atmospheric aerosol on climate, visibility and photochemistry requires knowledge of their optical and physical properties, such as the light extinction coefficient (the sum of the aerosol light scattering and absorption coefficients), Aerosol optical depth (AOD), single scattering albedo (ratio of scattering to extinction coefficients), upscatter fraction (fraction of incident solar radiation that is scattered upward to space), and size distribution [12 - 15].

Determination of AOD at different spectral wavelengths helps in deriving information on the optical properties and size distribution of particles, as well as studying the diurnal and season variability of aerosols [16].

Aerosol optical properties can be strongly dependent upon relative humidity (RH) becausewater uptake affects aerosol

Corresponding author: ***B. I. Tijjani,*** E-mail: idrith@yahoo.com, Tel. +234 8037030877

atmospheric lifetime and composition, which in turn affect atmospheric visibility and direct radiative forcing of climate [7]. The absorption of water by atmospheric aerosols with increasing relative humidity (RH) influences their size, composition, lifetime, chemical reactivity, light scattering and other optical and microphysical characteristics. Water is the most prevalent aerosol component at RHs above 80% and is often a significant component at lower RHs [17]. Accordingly, hygroscopic growth is important in a number of air pollution problems, including visibility impairment, climate effects of aerosols, acid deposition, long-range transport, and the ability of particles to penetrate into the human respiratory system. Aerosol optical properties depend on particle size and composition, which can be greatly influenced by hygroscopic growth [18, 19].

In this paper OPAC was used to model the effect of soot on optical depths, single scattering albedo and asymmetric parameter at eight different RHs (0, 50, 70, 80, 90, 95, 98 and 99%) at the spectral interval of 0.25μm to 1.00μm for urban aerosols, to determine its effect on the RF of urban aerosols. The optical depth was used to determine the Angstrom parameters to help us to see its effect on the particle size distributions and change in mode size distributions. Using regression analysis, the Angstrom exponents were determined along with α_1 and α_2, the coefficients of a second order polynomial fit.Finally, asymmetric parameters were also used to see its effect particle size and consequently in forward scattering.

The models extracted from OPAC are given in Table 1.

Table 1 Compositions of aerosol types [20].

Components	Model1(N_i,cm^{-3})	Model2(N_i,cm^{-3})	Model3(N_i,cm^{-3})
Insoluble	1.50	1.50	1.50
water soluble	15,000.00	15,000.00	15,000.00
Soot	110,000.00	120,000.00	130,000.00
Total	125,001.50	135,000.00	145,001.50

Although a fully exact radiative transfer model is difficult, so in this paper we used the approach of [21] where they show that the direct aerosol radiative forcing at the top of the atmosphere can be approximated by

$$\Delta F_R = -\frac{S_0}{4} T_{atm}^2 (1 - N_{cloud}) 2\tau\{(1-A)^2\beta\omega - 2A(1-\omega)\} \quad (1)$$

Where S_0 =1368Wm^{-2} is a solar constant, T_{atm} =0.79 is the transmittance of the atmosphere above the aerosol layer, N_{cloud}=0.6 is the fraction of the sky covered by clouds, the global averaged albedo A=0.22 over land, ω is the average single scattering albedo, β is the fraction of radiation scattered by aerosol into the atmosphere and τ the optical thickness [22]. The above expression gives the radiative forcing due to the change of reflectance of the earth-aerosol system. The upscattering fraction is calculated using an approximate relation [23].

$$\beta = \frac{1}{2}(1 - g) \quad (2)$$

where g is the asymmetry parameter. Although the model is simple but was used to provide reasonable estimates for the radiative forcing by both sulfate aerosols [24] and absorbing smoke aerosols [21].

The spectral behavior of the aerosol optical thickness, with the wavelength of light (λ) is expressed as inverse power law [25]:

$$\tau(\lambda) = \beta\lambda^{-\alpha} \quad (3)$$

where β is the turbidity and α is the Angstom exponent [26, 27]. The formula is derived on the premise that the extinction of solar radiation by aerosols is a continuous function of wavelength, without selective bands or lines for scattering or absorption [28]. The wavelength dependence of τ(λ) can be characterized by the Angstron parameter, which is a coefficient of the following regression:

$$\ln\tau(\lambda) = -\alpha\ln(\lambda) + \ln\beta \quad (4)$$

The Angstrom exponent itself varies with wavelength, and a more precise empirical relationship between aerosol extinction and wavelength is obtained with a 2nd-order polynomial [29-39]. as:

$$\ln\tau(\lambda) = \alpha_2(\ln\lambda)^2 + \alpha_1\ln\lambda + \ln\beta \quad (5)$$

Here, the coefficient α_2 accounts for a "curvature" often observed in sunphotometry measurements. In case of negative curvature (α_2<0, convex type curves) the rate of change of α is more significant at the longer wavelengths, while in case of positive curvature (α_2>0, concave type curves) the rate of change of α is more significant at the shorter wavelengths [34, 30, 31, 40]. [30]reported the existence of negative curvatures for fine-mode aerosols and positive curvatures for significant contribution by coarse-mode particles in the size distribution.

2.0 Results and Observations

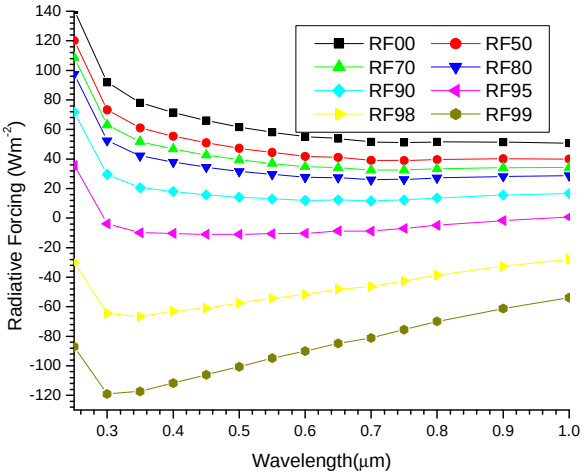

Figure 1a.A graph of radiative forcing against wavelength for model 1 at RHs 0, 50, 70, 80, 90, 95, 98 and 99%.

The graph shows that RF behaves as inverse power law with wavelength at RHs 0 to 70 but started curving upward (concave) at higher wavelengths from 80 and the curving continues to increase upto 99%. Its relation with RH is that RF(cooling) increases with the increase in RHs. It also shows that smaller particles have more impact on RF as the RH increases.

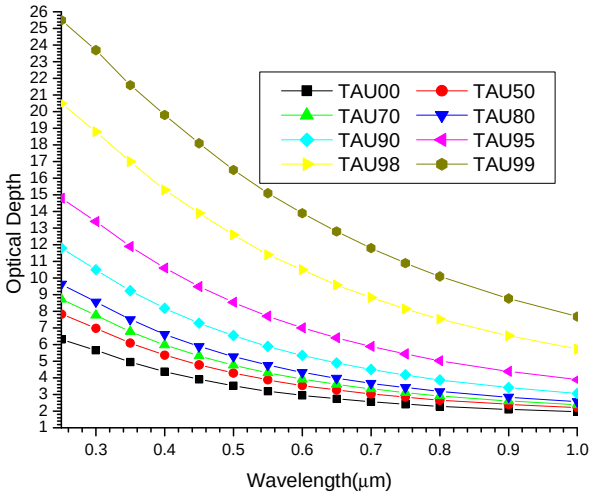

Figure 1b A graph of optical depth against wavelength for model 1 at RHs 0, 50, 70, 80, 90, 95, 98 and 99%.

The optical depth follows a relatively smooth decrease with wavelength for all RHs and can be approximated with power law wavelength dependence (equation (3)). It is evident from the figure that there is relatively strong wavelength dependence of optical depth at shorter wavelengths that gradually decreases towards longer wavelengths irrespective of the RH, attributing to the presence of fine and coarse particles. The presence of a higher concentration of the fine-mode particles which are selective scatters enhance the irradiance scattering in shorter wavelength only, while the coarse-mode particles provide similar contributions to the AOD at both wavelengths [41]. The relation with RH shows that hygroscopic growth has more effect on fine particles than coarse particles and also that has caused increase in mode size distributions. The relation of optical depth with RH is such that at the deliquescence point (90 to 99%) this growth with higher humidities increases substantially, making this process strongly nonlinear with relative humidity [42, 43]. A higher RH could obviously cause the particles' hygroscopic increase, which could result in greater extinction and a larger volume of fine particles and therefore increase in optical depth.

Table 2 The results of the Angstrom coefficients for Model1 using equations (4) and (5) at the respective relative humidities using regression analysis with SPSS16.0.

	Linear			Quadratic			
RH(%)	R^2	α	β	R^2	α_1	α_2	β
0	0.99716	0.88942	1.89869	0.99718	-0.87478	0.01074	1.90477
50	0.99767	0.95463	2.18600	0.99807	-1.01951	-0.04759	2.15528
70	0.99731	0.97719	2.37797	0.99839	-1.08704	-0.08058	2.32166
80	0.99666	0.99232	2.59259	0.99868	-1.14479	-0.11185	2.50777
90	0.99444	1.00563	3.15204	0.99913	-1.24161	-0.17311	2.99387
95	0.99054	0.99513	4.10309	0.99951	-1.31856	-0.23726	3.82356
98	0.98330	0.94069	6.21860	0.99982	-1.35728	-0.3056	5.67836
99	0.97709	0.88316	8.44252	0.99991	-1.34429	-0.33827	7.63453

Table 2 shows that at 0% RH the value of α from the linear part reflects the dominance of coarse particles (because $\alpha<1$), and the quadratic part also verifies this because $\alpha_2>0$. However as the RH increases from 50 to 90% the value of α continues to increase and α_2 becomes negative and the magnitude of α_2 continues to increase with the increase in RH which indicates the increase in the concentrations of fine particles with the increase in RH.

At the RH between 95 to 99% the value of α started decreasing, which implies that particles at the delinquent points appear to be large particles, because of swelling of water vapor and aging processes, exhibiting thus similar characteristics to the particles produced in arid areas [44, 45] but it can be observed that α_2 continued to increase, and this shows that at delinquent points increase in α_2 does not reflect increase in fine mode particles.

The observed variations in Ångström coefficients can be explained by changes in the effective radii of the mixtures resulting from changes in RH in the range 0% to 90%: the larger the number of small aerosol particles, the smaller the effective radius and the larger the Ångström coefficient The Ångström exponent increases with the increase in water vapor, which means that the effective radius of the aerosol particles become smaller when the water vapor increases. An increase in AOD with an increasing α as a result of change in RH, reflects the presence of a significant fraction of fine particles in the aerosol size distribution.

But as from 95% to 99% RH there is an increase in fine mode particle radius which results from particle growth due to coagulation and hygroscopic growth. Coagulation rates increase as particle concentration increases [40]; therefore this particle growth mechanism will be greatest at the highest optical depth (τ(λ)). Hygroscopic at high RH will also tend to increase optical depth as accumulation mode particles increase in size [46]. The high AOD is linked to a hygroscopic and/or coagulation growth from the fine aerosols. Furthermore, the fine mode aerosols have hydrate and coagulated characters that become large particles, causing the AOD to increase and α becomes smaller. Also the decrease in α as AOD increases, suggest the presence of larger particles leads to enhanced extinction. There is observational evidence that Ångström exponents decrease in value as particles grow hygroscopically[47].

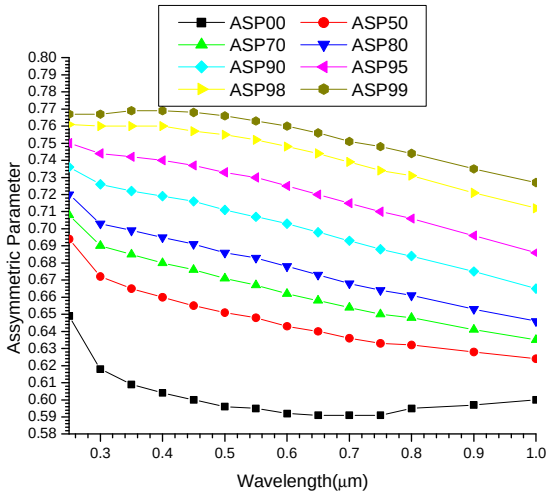

Figure 1c A graph of asymmetric parameter against wavelength for model 1 at RHs 0, 50, 70, 80, 90, 95, 98 and 99%.

The behavior of asymmetric parameter with wavelength is like power law but as it can be seen from the graph, the coefficient increases with the increase in RH (0%–90%) but becomes linear and increase with RH as from 95% – 99%. The increase of asymmetric parameter with RH shows that hygroscopic growth by particles as a result of increase in RH enhances scattering more in the forward direction of which that is why we have increase in RF(cooling) with RH.

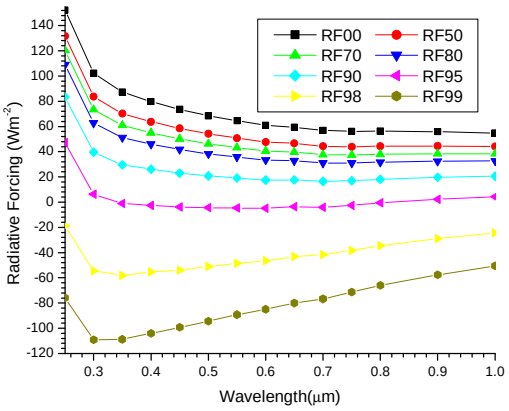

Figure2a A graph of radiative forcing against wavelength for model 2 at RHs 0, 50, 70, 80, 90, 95, 98 and 99%.

Figure 2a is almost similar to Figure 1a, but the main difference is that there is an increase in warming and continues to increase with the increase in RH.

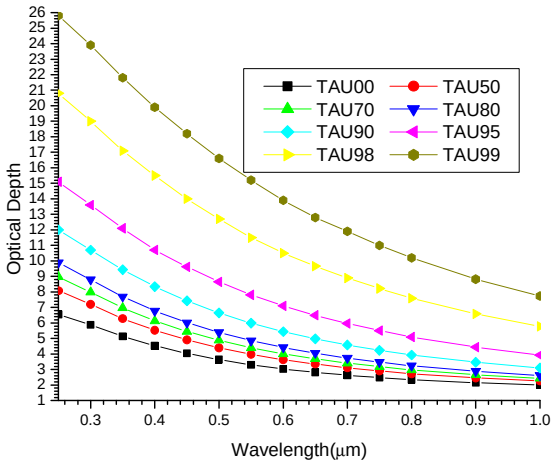

Figure 2b.A graph of optical depth against wavelength for model 2 at RHs 0, 50, 70, 80, 90, 95, 98 and 99%.

Figures 1b and 2b are similar for relation with wavelength, but there is a slight increase of optical depth with the increase in RH.

Table 3*The results of the Angstrom coefficients for Model2 using equations (4) and (5) at the respective relative humidities using regression analysis with SPSS16.0.*

	Linear			Quadratic			
RH(%)	R^2	α	β	R^2	α_1	α_2	β
0	0.99715	0.90177	1.943251	0.99716	-0.8917	0.007389	1.947526
50	0.99760	0.96343	2.230815	0.99803	-1.03138	-0.04985	2.197988
70	0.99726	0.98463	2.422911	0.99836	-1.09634	-0.08194	2.36458
80	0.99664	0.99871	2.637723	0.99865	-1.15178	-0.11229	2.551095
90	0.99451	1.01104	3.196606	0.99910	-1.2457	-0.17214	3.037081
95	0.99070	0.99927	4.147965	0.99950	-1.32093	-0.23596	3.866873
98	0.983532	0.94394	6.263338	0.99980	-1.35874	-0.30429	5.721444
99	0.977451	0.88640	8.485223	0.99991	-1.34539	-1.34539	7.676742

Comparing Table 3 with Table2, shows that values of α have increased, however for α_2, its value at 0% RH has decreased but at the remaining RH it has increased in magnitude.

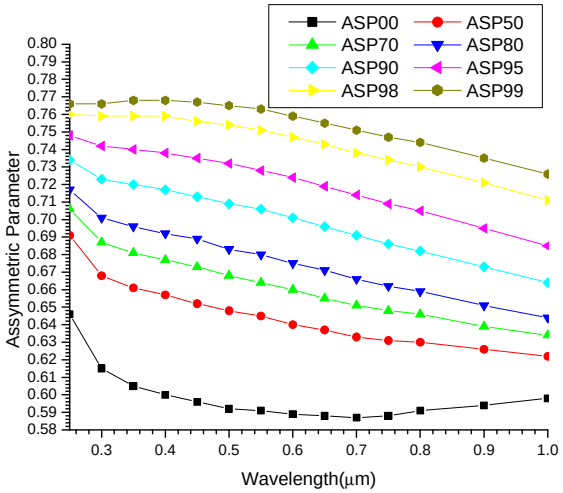

Figure 2c A graph of asymmetric parameter against wavelength for model 2 at RHs 0, 50, 70, 80, 90, 95, 98 and 99%.

Figure 2cand Figure 1c are similar in relation to wavelength, but in relation to RH shows that there is a slight decrease in asymmetric parameters.

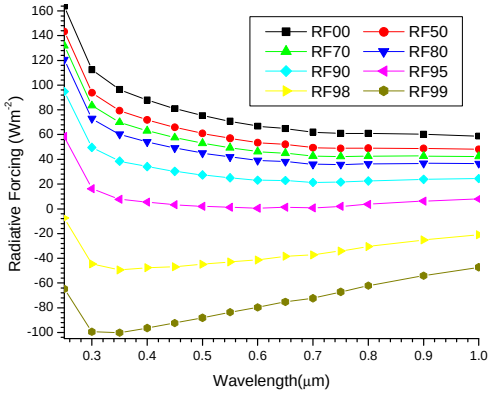

Figure 3a.A graph of radiative forcing against wavelength for model 3 at RHs 0, 50, 70, 80, 90, 95, 98 and 99%.

Figure 3a is similar to that of figures 1a and 2a in relation to wavelength, but shows an increase in warming and increases more with the increase in RH.

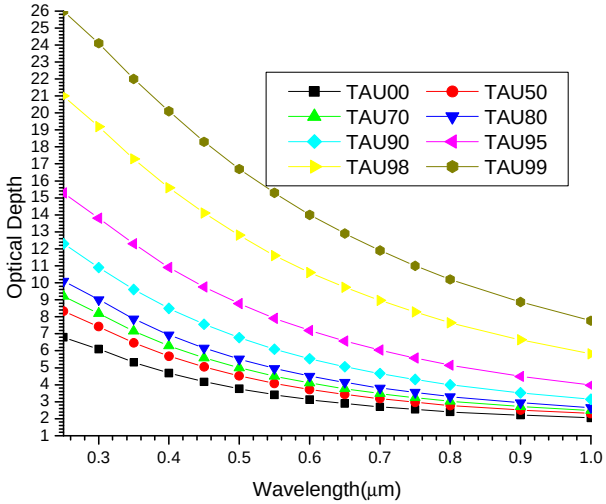

Figure 3b: A graph of optical depth against wavelength for model 3 at RHs 0, 50, 70, 80, 90, 95, 98 and 99%.

Figure 3b is similar to Figures 1b and 2b in relation to wavelength, but there is a slight increase in optical depth with respect to RHs.

Table 4The results of the Angstrom coefficients for Model3 using equations (4) and (5) at the respective relative humidities using regression analysis with SPSS16.0.

	Linear			Quadratic			
RH(%)	R^2	α	B	R^2	α_1	α_2	B
0	0.99714	0.91350	1.98778	0.99714	-0.90855	0.00363	1.98992
50	0.99755	0.97173	2.27574	0.99800	-1.04255	-0.05196	2.24085
70	0.99721	0.99172	2.46781	0.99833	-1.10516	-0.08322	2.40748
80	0.99664	1.00504	2.68255	0.99863	-1.15845	-0.11253	2.59426
90	0.99456	1.01606	3.24145	0.99908	-1.25010	-0.17168	3.08011
95	0.99084	1.00343	4.19279	0.99947	-1.32329	-0.23464	3.91019
98	0.98381	0.94737	6.30763	0.99979	-1.35989	-0.30261	5.76477
99	0.97783	0.88921	8.53057	0.99990	-1.34568	-0.33485	7.72200

The values of αs are higher than those of Tables 2 and 3. In relation to α_2, it decreases at 0 compared to the other two tables. But at higher RHs the α_2s are higher in magnitude than the corresponding α_2s of the other tables.

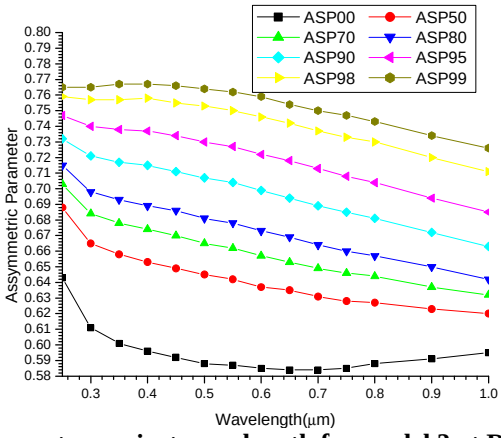

Figure 3c: A graph of asymmetric parameter against wavelength for model 3 at RHs 0, 50, 70, 80, 90, 95, 98 and 99%.

Figure 3c is similar to Figures 1c and 2c with respect to wavelength, but there is a slight decrease at all RHs compared to the two figures at the respective RHs.

CONCLUSIONS

From the figures of the RFs it can be observed that the increase in soot has caused an increase in RF in the form of warming. This is also verified by the decrease in asymmetric parameter because it reflects the decrease in forward scattering which automatically implied increase in absorption, so that is why we have increase in warming.The increase in α with the increase in soot reflects the increase in fine particles, which is also verified by the decrease in the positive curvatures (that is α_2) at 0% RH and increase in the negative of curvatures at the remaining RHs.

Also according to Schuster et al. [41], the absolute value of the coefficient α_1 decreases with increasing particle size for fine monomodal aerosols, but in our case it is observed that α_1 increases with the increase in soot and RHs, so this shows a sign of bimodal type of size distributions.

References

[1] Seinfeld, J.H and Pandis, S.N (1998), Atmospheric Chemistry and Physics from air pollution to climate change, John Wiley, Hoboken, N.J

[2] Jacobson, M. Z.(2001): Strong radiative heating due to the mixing state of black carbon in atmospheric aerosols, Nature, 409, 695–697.

[3] Salako, G.O., Hopke, P.K., Cohen, D.D., Begum, B.A., Biswas, S.K., Pandit, G.G., Chung, Y.S., Rahman, S.A., Hamzah, M.S., Davy, P., Markwitz, A., Shagjjamba, D., Lodoysamba, S., Wimolwattanapun, W. and Bunprapob, S. (2012). Exploring the Variation between EC and BC in a Variety of Locations. Aerosol Air Qual. Res. 12: 1–7.

[4] Hansen, J.E. and Sato, M. (2001). Trends of Measured Climate Forcing Agents. Proc. Nat. Acad. Sci. U.S.A. 98: 14778–14783.

[5] Menon, S., Hansen, J.E., Nazarenko, L. and Luo, Y. (2002). Climate Effects of Black Carbon Aerosols in China and India.Science 297: 2250–2253.

[6] Myhre, G., Stordal, F., Restad, K. and Isaksen, I.S.A. (1998). Estimation of the Direct Radiative Forcing Due to Sulfate and Soot Aerosols.Tellus Ser. B 50: 463–477.

[7] IPCC (2007), Climate Change 2007:Th e Physical Science Basis . Contribution of Working Group I to the Fourth Assessment Report of the Intergovernmental Panel on Climate Change, edited by S. Solomon et al., Cambridge Univ. Press, Cambridge, U. K.

[8] Chameides, W.L., Yu, H., Liu, S.C., Bergin, M., Zhou, X., Mearns, L., Wang, G., Kiang, C.S., Saylor, R.D., Luo, C., Huang, Y., Steiner, A. and Giorgi, F. (1999). Case Study of the Effects of Atmospheric Aerosols and Regional Haze on Agriculture: An Opportunity to Enhance Crop Yields in China through Emission Controls? Proc. Nat. Acad. Sci. U.S.A. 96: 13626–13633.

[9] Bergin, M., Greenwald, R., Xu, J., Berta, Y. and Chemeides, W.L. (2001). Influence of Aerosol Dry Deposition on Photosynthetically Active Radiation Available to Plants: A Case Study in the Yangtze Delta Region of China. Geophys. Res. Lett. 28: 3605–3608.

[10] Brown, L.M., Harrison, R. M., Maynard, A. D and Maynard, R. I (2003) Ultrafine particles in the atmosphere, London: Imperial College press.

[11] Gelencser, A (2005) Carbonaceous Aerosol. Dodrecht, the Netherland springer.

[12] Waggoner, A. P., Weiss, R. E., Ahlquist, N. C., Covert, D. S., Will, S., and Charlson, R. J.: Optical characteristics of atmospheric aerosols, Atmos. Environ., 15, 1891–1909, 1981.

[13] Haywood, J. and Boucher, O.: Estimates of the direct and indi-rectradiative forcing due to tropospheric aerosols: a review, Rev. Geophys., 38, 513-543, 2000.

[14] Alados-Arboledas, A., Alc´antara, A., Olmo, F. J., Mart´ınez-Lozano, J. A., Estell´es, V., Cachorro, V., Silva, A. M., Horvath, H., Gangl, A., D´ıaz, A., Pujadas, M., Lorente, J., Labajo, A., Sorribas, M., and Pavese, G.: Aerosol columnar properties retrieved from Cimel radiometers during VELETA 2002, Atmos. Environ., 42, 2630–2642, 2008.

[15] Alados-Arboledas, L., Lyamani, H., and Olmo, F. J.: Aerosol size properties at Armilla, Granada (Spain), Q. J. Roy. Meteor.Soc., 129, 1395–1413, 2003.

[16] Rana S., Kant Y., Dadhwal V. K. (2009), *Diurnal and Seasonal Variation of Spectral Properties of Aerosols over Dehradun, India* Aerosol and Air Quality Research, Vol. 9, No. 1, pp. 32-49, 2009

[17] Hanel, G. (1976). The Properties of Atmospheric Aerosol Particles as Functions of Relative Humidity at Thermodynamic Equilibrium with Surrounding Moist Air. In *Advances in Geophysics, Vol. 19*,H. E. Landsberg and J.VanMieghem, eds., Academic Press, New York, pp. 73–188.

[18] Mikhailov, E. F., Vlasenko, S. S., Podgorny, I. A., Ramanathan, V., and Corrigan, C. E.: Optical properties of soot-water drop agglomerates: An experimental study, J. Geophys. Res.-Atmos., 111, D07209, doi:10.1029/2005Jd006389, 2006.

[19] Garland, R. M., Ravishankara, A. R., Lovejoy, E. R., Tol-bert, M. A., and Baynard, T.(2007): Parameterization for the relative humidity dependence of light extinction: Organic-ammonium sulfate aerosol, J. Geophys. Res.-Atmos., 112, D19303, doi:10.1029/2006JD008179.

[20] Hess M., Koepke P., and Schult I. (May 1998), Optical Properties of Aerosols and Clouds: The Software Package OPAC, Bulletin of the A merican Met. Soc. **79**, 5, p831-844.

[21] Chylek, P., and J. Wong (1995), Effect of absorbing aerosols on global radiation bud get, Geophys . Res. Lett. , 22(8), 929 – 931, doi: 10.1 029/95GL00800.

[22] Penner, J. E., Dickinson, R. E. and O'Neil, C. A. (1992). Effects of aerosol from biomass burning on the global radiation budget. Science 256, 1432-1434.

[23] Segan, C. and Pollack, J. (1967). Anisotropic nonconservative scattering and the clouds of Venus. J. Geophys. Res. 72, 469-477.

[24] Charlson, R.J., Schwartz, S.E., Hales, J. M., Cess, R. D., Coakley, J. A., Hansen, J. E and Hotmann, D. J (1992) Climate forcing by anthropogenic aerosols, Science 255, 423-430

[25] Ångström, A.K. (1961). Techniques of Determining the Turbidity of the Atmosphere.Tellus XIII: 214.

[26] Liou K. N.(2002) An Introduction to Atmospheric Radiation, 2nd ed. Academic, San Diego, Calif.,.

[27] O'Neill, N. T and Royer, A (1993): Extraction of Binomial aerosol-size distribution Radii From spectral and angular slope (Angstrom) coefficients *App Opt*. 32 1642-1645.

[28] Ranjan, R.R., Joshi, H.P. and Iyer, K.N. (2007). Spectral variation of total column aerosol optical depth over Rajkot: A tropical semi-arid Indian station. Aerosol Air Qual. Res. 7: 33-45.

[29] King, M. D. and Byrne, D. M.: A method for inferring total ozone content from spectral variation of total optical depth obtained with a solar radiometer, J. Atmos. Sci., 33, 2242–2251, 1976.

[30] Eck, T. F., Holben, B. N., Reid, J. S., Dubovic, O., Smirnov, A., O'Neil, N. T., Slutsker, I., and Kinne, S.: Wavelength dependence of the optical depth of biomass burning, urban, and desert dust aerosols, J. Geophys. Res., 104(D24), 31 333–31 349, 1999.

[31] Eck, T. F., Holben, B. N., Ward, D. E., Dubovic, O., Reid, J. S., Smirnov, A., Mukelabai, M. M., Hsu, N. C., O' Neil, N. T., and Slutsker, I.: Characterization of the optical properties of biomass burning aerosols in Zambia during the 1997 ZIBBEE field campaign, J. Geophys. Res., 106(D4), 3425–3448, 2001.

[32] Eck, T. F., Holben, B. N., Dubovic, O., Smirnov, A., Slutsker, I., Lobert, J. M., and Ramanathan, V.: Column-integrated aerosol optical properties over the Maldives during the northeast mon-soon for 1998–2000, J. Geophys. Res., 106, 28 555–28 566, 2001.

[33] Eck, T. F., Holben, B. N., Ward, D. E., et al.: Variability of biomass burning aerosol optical characteristics in southern Africa during SAFARI 2000 dry season campaign and a compari-son of single scattering albedo estimates from radiometric measurements, J. Geophys. Res., 108(D13), 8477, doi:10.1029/2002JD002321, 2003

[34] Kaufman, Y. J., Aerosol optical thickness and atmospheric path radiance, J. Geophys. Res., 98, 2677-2992, 1993.

[35] O'Neill, N. T., Dubovic, O., and Eck, T. F.(2001): Modified˚ Angstrom exponent for the characterization of submicrometer aerosols, Appl. Opt., 40(15), 2368–2375.

[36] O'Neill, N. T., Eck, T. F., Holben, B. N., Smirnov, A., and Dubovic, O.: Bimodal size distribution influences on the variation of ˚ Angstr¨ omderivates in spectral and optical depth space, J. Geophys. Res., 106(D9), 9787–9806, 2001.

[37] O'Neill, N. T., Eck, T. F., Smirnov, A., Holben, B. N., and Thulasiraman, S.: Spectral dis-crimination of coarse and fine mode optical depth, J. Geophys. Res., 198(D17), 4559, doi:101029/2002JD002975, 2003.

[38] Pedros, R., Martinez-Lozano, J. A., Utrillas, M. P., Gomez-Amo, J. L., and Tena, F.(2003): Column-integrated aerosol, optical properties from ground-based spectroradiometer measurements at Barrax (Spain) during the Digital Airborne Imaging Spectrometer Experiment (DAISEX) campaigns, J. Geophys. Res., 108(D18), 4571, doi:10.1029/2002JD003331,.

[39] Kaskaoutis, D. G. and Kambezidis, H. D.(2006): Investigation on the wavelength dependence of the aerosol optical depth in the Athens area, Q. J. R. Meteorol. Soc., 132, 2217–2234,.

[40] Reid, S. J., Eck T. F., Christopher S. A., Hobbs P. V. and Holben B.,(1999) Use of Angtrom exponent to estimate the variability of optical and physical properties of aging smoke particles in Brazil, J. Geophys. Res. 104(D22), 27, 473—27, 489.

[41] Schuster, G. L., Dubovik, O., and Holben, B. N.: Angstrom exponent and bimodal aerosol size distributions, J. Geophys. Res., 111, D07207, doi:101029/2005JD006328, 2006.

[42] Fitzgerald, J. W. (1975) Approximation formulas for the equilibrium size of an aerosol particle as a function of its dry size and composition and ambient relative humidity. J. Appl. Meteorol., 14, 1044 –1049

[43] Tang, I. N. (1996). Chemical and size effects of hygroscopic aerosols on light scattering coefficients. Journal of Geophysical Research, 101, 19245–19250.

[44] Kaskaoutis D. G., Kambezidis H. D., Hatzianastassiou N., Kosmopoulos P. G., and Badarinath K. V. S. (2007) Aerosol climatology: dependence of the Angstrom exponent on wavelength over four AERONET sites, Atmos. Chem. Phys. Discuss., 7, 7347–7397.

[45] Kaskaoutis, D. G., Kambezidis, H. D., Hatzianastassiou, N., Kosmopoulos, P. G., &Badarinath, K. V. S. (2007). Aerosol climatology: On the discrimination of aerosol types over four AERONET sites. Atmospheric Chemistry and Physical Discussion, 7,6357−6411.

[46] Eck, T. F., Holben, B. N., Dubovic, O., Smirnov, A., Goloub, P., Chen, H. B., Chatenet, B., Gomes, L., Zhang, X. Y., Tsay, S. C., Ji, Q., Giles, D., and Slutsker, I.: Columnar aerosol optical properties at AERONET sites in central eastern Asia and aerosol transport to the tropical mid-Pacific, J. Geophys. Res., 110, D06202, doi:10.1029/2004JD005274, 2005.

[47] Carrico, C.M., Rood, M.J., Ogren, J.A., (1998): Aerosol light scattering properties at Cape Grim, Tasmania, during the First Aerosol Characterization Experiment (ACE 1), J. Geophys. Res ., 103, 16565-16574.